Discussion Paper Series
No. Ⅰ -119

Predictability of Chaotic Dynamics in a Regime-Switching Solow Model

Jing Zhang, Masanori Yokoo
October 29, 2024

Predictability of Chaotic Dynamics in a Regime-Switching Solow Model*

Jing Zhang† Masanori Yokoo‡

October 29, 2024

Abstract

In this paper, we modify the discrete-time Solow model by introducing technology choice and imperfect observation to generate chaotic endogenous business cycles. In particular, we specify the parameters under which the model satisfies the Markov property to show that the chaotic behavior is predictable in the sense that the stationary distribution of the dynamics is explicitly represented.

JEL classification: C63, E32, O14, O41.
Keywords: Piecewise linear Solow model; Technology choice; Observation errors; Endogenous cycles; Chaotic dynamics; Markov property

*This research is financially supported by the Grants-in-Aid for Scientific Research, JSPS (21K01388).
†Graduate School of Humanities and Social Sciences, Okayama University, Tsushimanaka 3-1-1, Kita-ku, Okayama 700-8530, Japan. e-mail: pazp80p3@s.okayama-u.ac.jp
‡Graduate School of Humanities and Social Sciences, and Faculty of Economics, Okayama University, Tsushimanaka 3-1-1, Kita-ku, Okayama 700-8530, Japan. e-mail: yokoo@e.okayama-u.ac.jp

1 Introduction

The global economy has experienced several boom-and-bust cycles over the past decades, and the mechanisms of such business cycles have been investigated extensively. Roughly speaking, there are traditionally two types of explanations for business cycles: exogenous and endogenous. In this context, recent studies, including Beaudry et al. (2020), provide empirical evidence that business cycle fluctuations are better explained by considering endogenous cycles than by external shocks alone.

On the other hand, the Solow model, the most familiar growth model in economics, has been used as a basic model in many fields of macroeconomics and is still widely applied. Based on a modified Solow model, for instance, Chen et al. (2014) proposed that dynamic convergence to a moving steady state exists, testing this with an empirical analysis of the U.S. economy. More recently, Kufenko et al. (2020) empirically examined predictions of the history-augmented Solow model concerning cross-country income inequality.

In addition to empirical studies, the Solow model is of great importance to theoretical analysis. Departing from the textbook Solow model, which is based on convergence to a steady state, there are modified Solow models that provide frameworks for analysis of *endogenous cycles*. Among the existing studies related to endogenous cycles, Böhm and Kaas (2000) incorporated different savings behaviors of shareholders and workers into the Solow model (called the Kaldor–Pasinetti model). They showed that cyclical, as well as chaotic, fluctuations can emerge when shareholders have a higher savings rate than workers. Quite recently, Agliari et al. (2020) extended the Kaldor–Pasinetti model to assume that overlapping generations of workers and capitalists have ownership of capital and revealed a wide range of bifurcations and complex dynamics. Sushko et al. (2020) explored border collision bifurcation in a modified Solow model in which capitalists' saving behavior influences that of workers.

Unlike Böhm and Kaas (2000), Agliari et al. (2020), and Sushko et al. (2020), we do not assume differential savings. Instead, we assume a switch of production technology. More specifically, shareholders of the firm can choose the production technology that maximizes their capital income. It is shown that this *technology choice* induces certain structural changes that generate strong threshold nonlinearities, resulting in cyclical dynamics in the Solow model.

Several recent studies have emphasized the mechanisms by which technology choice generates endogenous cycles. See Umezuki and Yokoo (2019) for two Cobb–Douglas technology choices and Asano et al. (2022) for Leontief and linear technology choices. Their theoretical explorations were based on overlapping generations (OLG) models. However, this paper attempts to consider technology choice in a Solow framework. We should not interpret this as a backward-looking application, because the Solow model is the most basic of many growth models (including the OLG model and the Ramsey model) and is not subject to the "one period is too long" criticism that Diamond's OLG model always receives.

In addition to technology choice, there is another important component of our setting: observation errors. Given the inherent uncertainty in observations of the economic environment, it is reasonable to consider observation errors. Especially, when faced with the choice of production technology, firms do not have sufficient information to make a decision. Yokoo and Ishida (2008) emphasized the role of observation errors in generating chaos in a macroeconomic model. Asano and Yokoo (2019) generated ergodic chaos by incorporating information imperfection into a Matsuyama-type credit cycle model. In both studies, observation errors add stronger nonlinearity to the threshold nonlinearity in the underlying models, resulting in chaotic dynamics.

Our goal in this paper is not so much to show that endogenous periodic or chaotic fluctuations occur in the Solow model from the introduction of technology choice and observation errors, but rather to describe the dynamics of chaotic fluctuations when they do occur, by deriving a stationary distribution of their dynamics using the *Markov property*. For this reason, the emphasis herein is not on the unpredictability of chaos, but rather on its *predictability*.

The rest of the paper is organized as follows. Section 2 introduces the model, in which binary technology choice and observable uncertainty are incorporated. Section 3 is devoted to a brief explanation of periodic fluctuations under perfect observation. Section 4 investigates the chaotic dynamics under imperfect observation, in which the chaotic trajectories are characterized by the Markov property. Section 5 gives some concluding remarks.

2 The model

We recapitulate the discrete version of the Solow's (1956) model. Time extends from 0 to infinity. A single commodity is produced from the input of labor L_t and capital K_t at constant returns to scale. Let $y_t = Y_t/L_t$ and $k_t = K_t/L_t$ be output and capital per worker, respectively, $n \geq 0$ denote the labor force growth rate, $\delta \in (0, 1]$ be the depreciation rate of capital, and $s \in (0, 1)$ be the saving rate. Then, the model formulation is as follows:

$$k_{t+1} = \frac{1}{1+n}[sf(k_t) + (1-\delta)k_t].$$

Now, departing from this standard growth model, we will consider switching the production technology and having observation errors of the economic state.

2.1 Binary choice of technology

First of all, we consider that two types of production technologies exist, one of which is Leontief type and the other is linear. Both are extreme cases of the constant elasticity of substitution (CES) production function. More specifically, the Leontief production function can be obtained by setting the elasticity of substitution between capital and labor to zero, whereas linear production technology can be derived by letting the elasticity of substitution approach infinity.

Following Asano et al. (2022), the two types of production technologies in intensive form are given by

$$y_t = f(k_t) = \begin{cases} f_1(k_t) = \begin{cases} A_1 k_t & \text{if} \quad k_t < 1, \\ A_1 & \text{if} \quad k_t \geq 1, \end{cases} \\ f_2(k_t) = A_2[\alpha k_t + (1-\alpha)], \end{cases}$$

where the subscripts 1 and 2 indicate the Leontief and linear technologies, respectively, $A_1, A_2 > 0$, and $\alpha \in (0, 1)$. It should be noted that the derivative of the Leontief production function does not exist at threshold $k = 1$. For the sake of simplicity, we will use the right-hand derivative of f_1 at $x = 1$ as $f_1'(1)$.

We assume that shareholders of the firm choose the technology that maximizes the capital income $kf'(k)$, or equivalently the marginal product of capital $f'(k)$ given k. That is, the firm only cares about achieving its highest return when deciding on the production technology. Thus, the first-order derivatives of the above production functions are given by

$$f'(k_t) = \begin{cases} f_1'(k_t) = \begin{cases} A_1 & \text{if} \quad k_t < 1, \\ 0 & \text{if} \quad k_t \geq 1, \end{cases} \\ f_2'(k_t) = \alpha A_2. \end{cases}$$

To prevent a scenario where the Leontief technology is never selected, it is assumed that $A_1 > \alpha A_2$. Namely, the Leontief technology is chosen for $k_t < 1$, and the linear technology is chosen for $k_t \geq 1$. The choice of production technology is illustrated in Fig. 1.

Given this binary choice of technology, the regime-switching model describing capital accumulation is given by

$$k_{t+1} = \begin{cases} \frac{1}{1+n}(sA_1 + 1 - \delta)k_t, & \text{if } k_t < 1, \\ \frac{1}{1+n}[(sA_2\alpha + 1 - \delta)k_t + sA_2(1-\alpha)], & \text{if } k_t \geq 1. \end{cases} \tag{1}$$

Clearly, this one-dimensional difference equation with a discontinuity depends on the parameters n, δ, s, A_1, A_2, and α. Moreover, there may exist four different typical dynamic behaviors relying on parameters, which are illustrated in Fig. 2.

It is obvious from Fig. 2 that case (a) converges to a unique positive steady state; case (b) exhibits permanent growth; case (c) converges to two locally stable steady states (the lower one corresponds to the poverty trap); and case (d) exhibits cyclical behavior. The dynamics occurring in cases (a), (b), and (c) are immediately clear; thus, it is much more interesting to examine case (d).

To simplify the presentation, we will introduce some new parameters as follows:

$$a = \frac{sA_1 + 1 - \delta}{1+n}, \qquad b = \frac{sA_2\alpha + 1 - \delta}{1+n}, \qquad c = \frac{sA_2(1-\alpha)}{1+n}.$$

Since we are interested in complex dynamics, we confine our analysis to case (d) where $a > 1 > b + c$, which is equivalent to

$$A_1 > \frac{n+\delta}{s} > A_2.$$

It is easy to confirm that the set of parameter values satisfying this inequality is non-empty. In addition, the above condition of technology switch $A_1 > \alpha A_2$ also holds under $a > 1 > b + c$.

Every trajectory generated by (1) will eventually enter the trapping interval $T = [b + c, a]$. Therefore, our focus will be on the dynamics of the following map:

$F : T \to T$,

$$k_{t+1} = F(k_t) = \begin{cases} ak_t \equiv F_L(k_t), & \text{if } k_t < 1, \\ bk_t + c \equiv F_R(k_t), & \text{if } k_t \geq 1. \end{cases} \tag{2}$$

Note that $b + c = (sA_2 + 1 - \delta)/(1 + n)$, which is independent of α. Additionally, a, b, and c can take any nonnegative values by appropriate choice of n, δ, s, A_1, A_2, and α.

By a straightforward change of variables

$$x_t = \frac{k_t - (b+c)}{a - (b+c)},$$

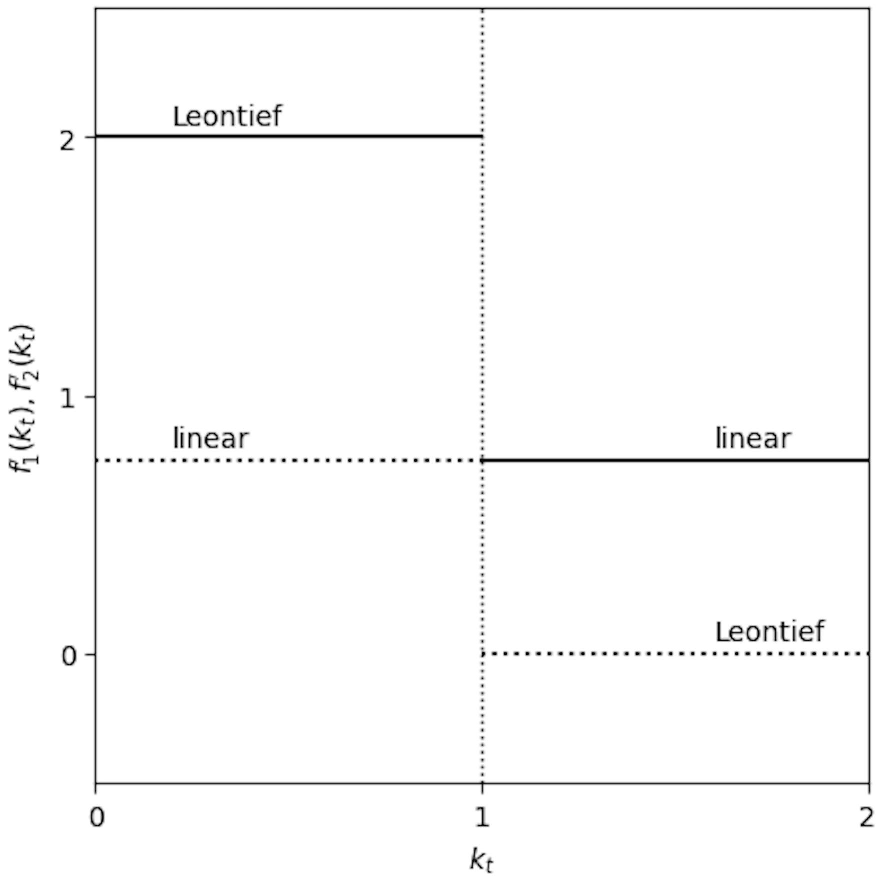

Figure 1: Binary choice of production technology. Solid lines indicate the chosen technologies. $A_1 = 2, A_2 = 1.5, \alpha = 0.5$.

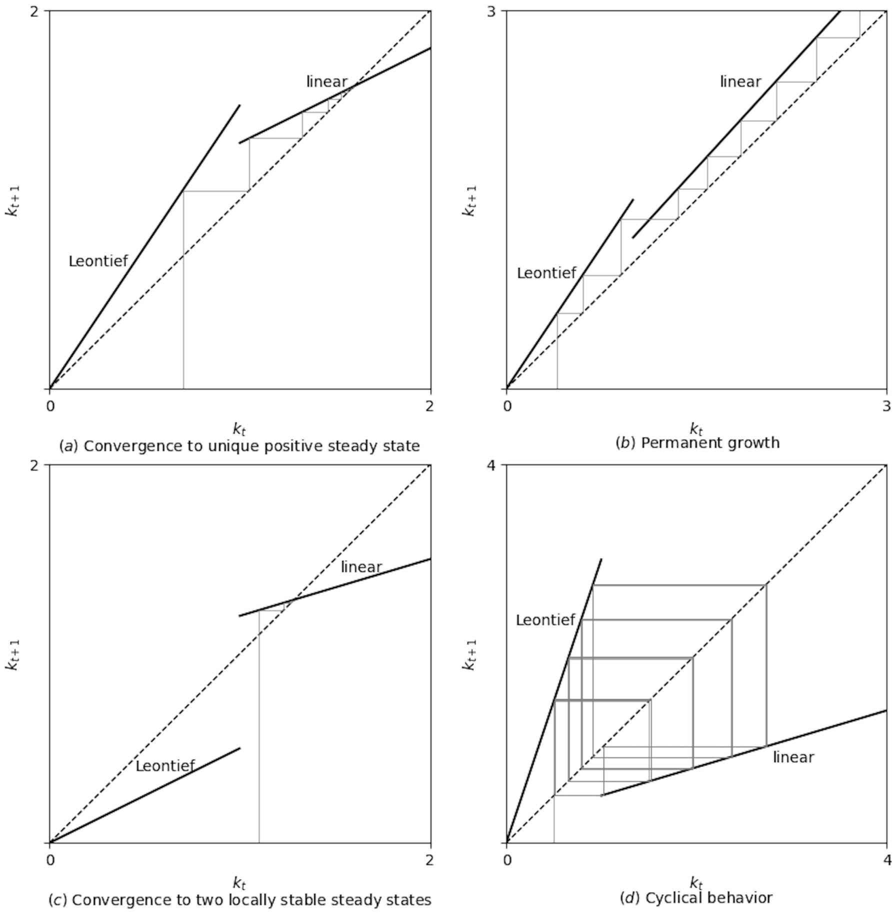

Figure 2: Different types of dynamic behavior. $n = 0, \delta = 1, s = 0.2$, $(a) A_1 = 7.5, A_2 = 6.5, \alpha = 5/13$, $(b) A_1 = 7.5, A_2 = 6, \alpha = 11/12$, $(c) A_1 = 2.5, A_2 = 6, \alpha = 0.25$, $(d) A_1 = 15, A_2 = 2.5, \alpha = 0.6$.

it is possible to transform the map F into the map $\tilde{\varphi}$, which maps the unit interval $I = [0, 1]$ into itself.

$\tilde{\varphi} : I \to I$,

$$x_{t+1} = \tilde{\varphi}(x_t) = \begin{cases} 1 + a(x_t - \theta) \equiv \tilde{\varphi}_L(x_t), & \text{if } 0 \leq x_t < \theta, \\ b(x_t - \theta) \equiv \tilde{\varphi}_R(x_t), & \text{if } \theta \leq x_t \leq 1, \end{cases} \tag{3}$$

where

$$\theta = \frac{1 - (b + c)}{a - (b + c)} = \frac{n + \delta - sA_2}{s(A_1 - A_2)} = \frac{n + \delta}{s(A_1 - A_2)} - \frac{A_2}{A_1 - A_2}.$$

One can easily confirm that θ can take any value between 0 and 1. See the appendix for a proof. Note also that there is an inverse relationship between θ and saving rate s. Fig. 3 depicts map $\tilde{\varphi}$, which has a jump discontinuity at θ and is increasing elsewhere.

2.2 Uncertainty of observation

Next, we take one more step forward. Firms cannot observe the true state variables with precision, due to insufficient information. Therefore, observation errors are explicitly considered in the regime-switching model of the previous subsection. Following Yokoo and Ishida (2008), we assume that state variables are observed with additive noise,

$$\hat{x}_{i,t} = x_t + \sigma\varepsilon_{i,t}.$$

Here, the observation $\hat{x}_{i,t}$ made by firm i at time t includes a disturbance term $\varepsilon_{i,t}$, which follows the cumulative distribution function G, has a zero mean, and is independent of t and i. $\sigma > 0$ is constant and measures the degree of uncertainty. In particular, $\sigma = 0$ indicates that there is no noise involved. Then, the probability of adopting the Leontief technology (technology 1) is

$$\text{Prob}\{\hat{x}_{i,t} < \theta\} = \text{Prob}\left\{\varepsilon_{i,t} < \frac{\theta - x_t}{\sigma}\right\} = G\left(\frac{\theta - x_t}{\sigma}\right).$$

The argument of the last term, $(\theta - x_t)/\sigma$, can be written as

$$\rho(k_t) = \frac{1 - k_t}{\sigma(a - b - c)}.$$

Here, we introduce the uncertainty of observation into the original model (2) and obtain the following general version of the difference equation:

$$k_{t+1} = [aG(\rho(k_t)) + b(1 - G(\rho(k_t)))]k_t + (1 - G(\rho(k_t)))c. \tag{4}$$

It can be easily confirmed that F_L of (2) can be obtained when $G(\rho(k_t)) = 1$ and F_R of (2) can be derived from $G(\rho(k_t)) = 0$. However, it is necessary to further specify $G(\rho(k_t)) \in (0, 1)$ from the final model.

We first define $G_M = G(\rho(k_t))$ for $G(\rho(k_t)) \in (0, 1)$. In general, $G(\rho(k_t))$ can be represented in the following form:

$$G(\rho(k_t)) = \begin{cases} 0 & \text{if} \quad \rho(k_t) < -1, \\ G_M & \text{if} \ -1 \leq \rho(k_t) < 1, \\ 1 & \text{if} \quad \rho(k_t) \geq 1. \end{cases} \tag{5}$$

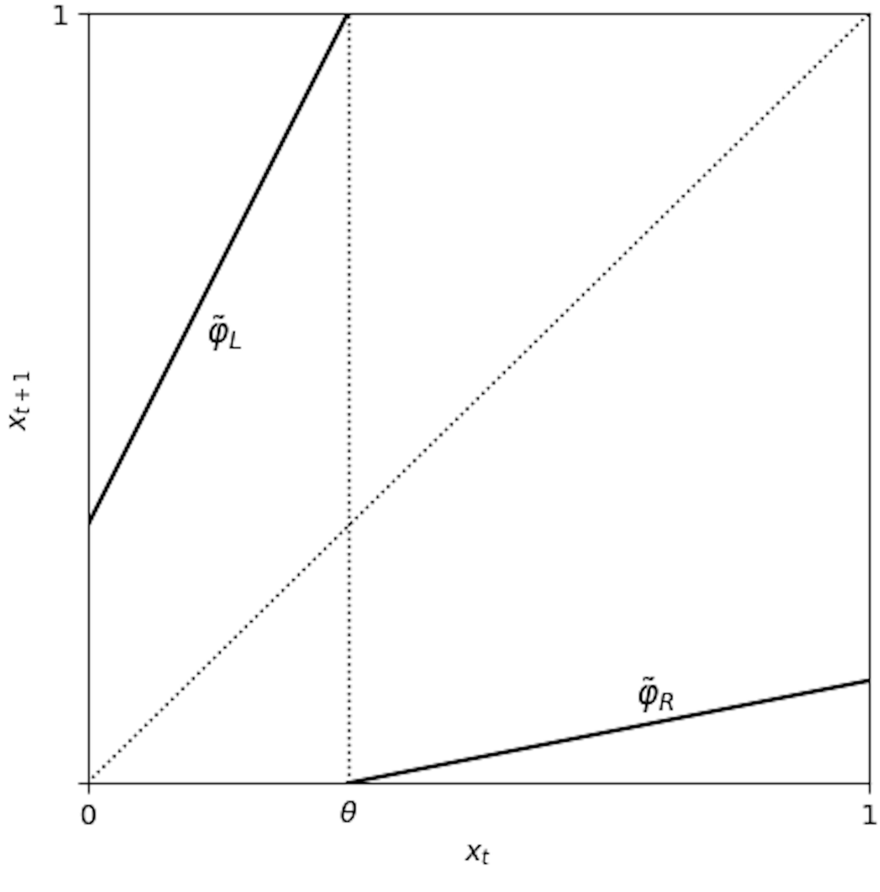

Figure 3: Graph of $\tilde{\varphi}(x_t)$. $n = 0, \delta = 1, s = 0.2, A_1 = 10, A_2 = 2.5, \alpha = 0.4$.

Furthermore, define k_L and k_R as the solutions of $\rho(k_L) = 1$ and $\rho(k_R) = -1$, respectively, for $\sigma > 0$ sufficiently small. Then, a simple computation shows that

$$k_L = 1 - \sigma(a - b - c), \qquad k_R = 1 + \sigma(a - b - c). \tag{6}$$

Note that $k_L < 1 < k_R$. It is clear that $\lim_{\sigma\to 0} k_L = \lim_{\sigma\to 0} k_R = 1$. Since capital per worker must be positive, we impose the condition that $k_L > 0$. This implies

$$0 < \sigma < \frac{1}{a - b - c} = \frac{1+n}{s(A_1 - A_2)}. \tag{7}$$

Subsequently, if G_M is appropriately specified, then dynamic equation (4) has a trapping interval $[bk_R + c, ak_L]$. By an analogous change of variables $h : [bk_R + c, ak_L] \to [0, 1]$ such that

$$x_t = h(k_t) = \frac{k_t - (bk_R + c)}{ak_L - (bk_R + c)},$$

it is possible to transform equation (4) into the following map:

$$x_{t+1} = \begin{cases} 1 + a(x_t - \theta_L), & \text{if } 0 \le x_t < \theta_L, \\ \varphi_M(x_t) & \text{if } \theta_L \le x_t < \theta_R, \\ b(x_t - \theta_R), & \text{if } \theta_R \le x_t \le 1, \end{cases}$$

where

$$\theta_L = \frac{k_L - (bk_R + c)}{ak_L - (bk_R + c)}, \qquad \theta_R = \frac{k_R - (bk_R + c)}{ak_L - (bk_R + c)}. \tag{8}$$

Note also that $\lim_{\sigma\to 0} \theta_L = \lim_{\sigma\to 0} \theta_R = \theta$, and $\varphi_M(x_t)$ depends on G_M. In order to make our model significantly tractable, we set

$$\varphi_M(x_t) = \frac{\theta_R - x_t}{\theta_R - \theta_L}.$$

Here, based on this form of $\varphi_M(x_t)$, it is possible to deduce the shape of G_M. That is, the explicit form of G_M could be obtained such that it satisfies the following equation:

$$[aG_M + b(1 - G_M))]\, k_t + (1 - G_M)c = h^{-1}(\varphi_M(h(k_t))).$$

If we let $y_t = \rho(k_t)$ and solve the above equation for $G_M(y_t)$, then we get

$$G_M(y_t) = \frac{(a-b)[1 - \sigma(a-b-c)] - c}{(a-b)[1 - \sigma(a-b-c)y_t] - c} \cdot \frac{1 + y_t}{2}. \tag{9}$$

See the appendix for the computation of G_M. It is also verified that $\lim_{y\to -1} G_M = 0$ and $\lim_{y\to 1} G_M = 1$. These values correspond exactly to equation (5), which is illustrated in Fig. 4.

Above, we have specified the functional form of G_M and obtained a piecewise linear function that maps the unit interval onto itself. For the reader's convenience, we rewrite the model that we will analyze in this paper as below.

$\varphi : I \to I$,

$$x_{t+1} = \varphi(x_t) = \begin{cases} 1 + a(x_t - \theta_L) \equiv \varphi_L(x_t), & \text{if } 0 \le x_t < \theta_L, \\ (\theta_R - x_t)/(\theta_R - \theta_L) \equiv \varphi_M(x_t) & \text{if } \theta_L \le x_t < \theta_R, \\ b(x_t - \theta_R) \equiv \varphi_R(x_t), & \text{if } \theta_R \le x_t \le 1. \end{cases} \tag{10}$$

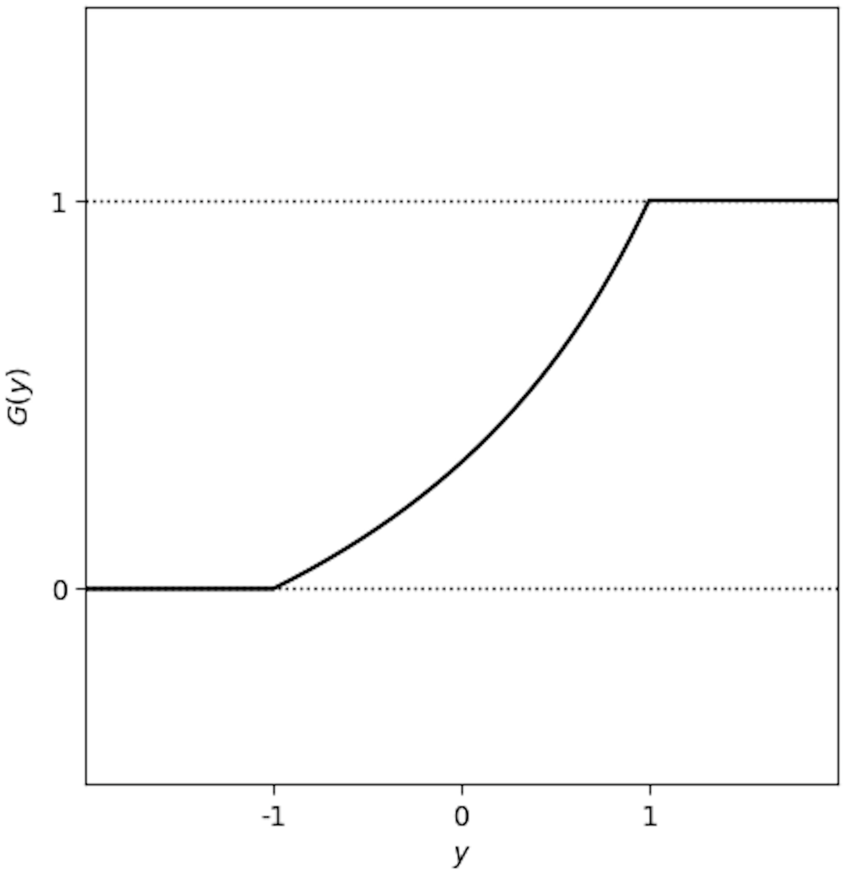

Figure 4: Graph of cumulative distribution function $G(y)$. $n = 0, \delta = 1, s = 0.2, A_1 = 20, A_2 = 3, \alpha = 5/6, \sigma = 0.1$.

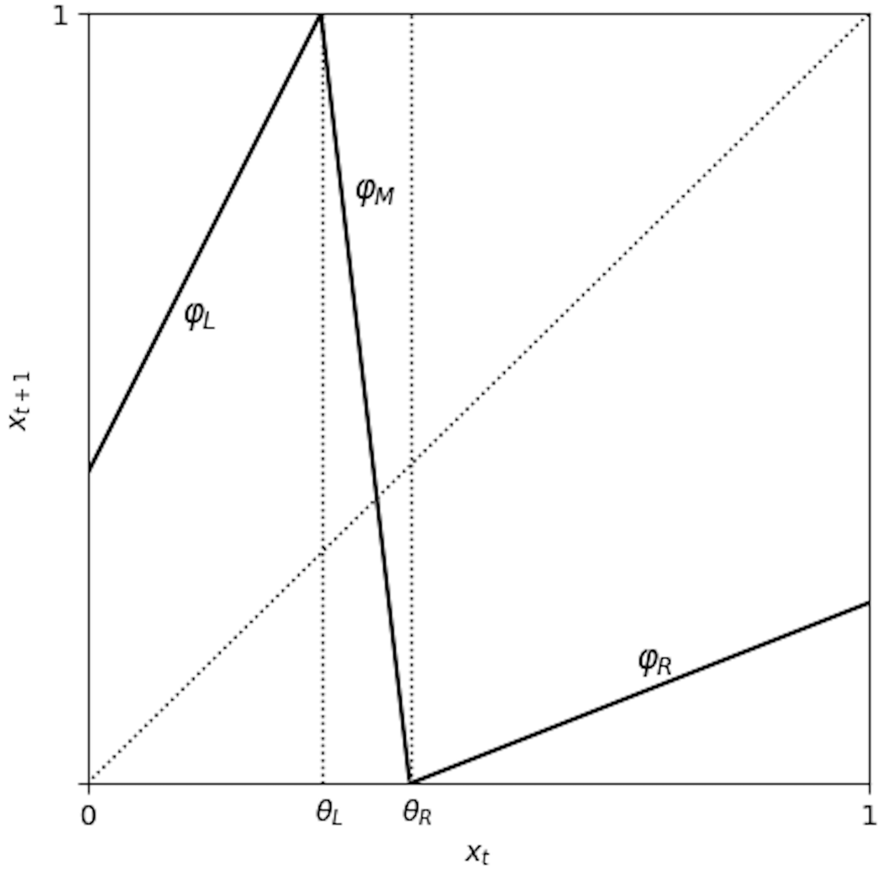

Figure 5: Graph of $\varphi(x_t)$. $n = 0, \delta = 1, s = 0.2, A_1 = 10, A_2 = 2.5, \alpha = 0.8, \sigma = 0.05$.

Fig. 5 shows that φ is N-shaped. Moreover, note that φ is influenced by σ and will evolve into $\tilde{\varphi}$ given by (3) when uncertainty disappears.

In the following, we will characterize the dynamics of the model given by (3) and (10). Depending on whether there is uncertainty or not, periodic cycles and chaotic behaviors are investigated. As indicated in the title of this paper, we intend to focus more on chaotic behaviors than periodic cycles.

3 Periodic fluctuations under perfect observation

Here, we briefly examine the dynamics of the model in the absence of noise or uncertainty. The model is represented by (3), which is a piecewise linear one-dimensional map with a jump discontinuity at θ. Under perfect observation, firms can accurately evaluate all relevant factors to select suitable production technologies. In fact, the dynamics of this specification of the model have been extensively investigated, for instance, by Keener (1980). In this case, we simply calculate $\tilde{\varphi}(0)$ and $\tilde{\varphi}(1)$:

$$\tilde{\varphi}(0) = \frac{(b+c)(a-1)}{a-(b+c)}, \qquad \tilde{\varphi}(1) = \frac{b(a-1)}{a-(b+c)}.$$

Since $\tilde{\varphi}(0) > \tilde{\varphi}(1)$, this corresponds to the nonoverlapping case considered by Keener(1980). Based on Keener's (1980) results, a mapping like (3) either exhibits periodic behavior or converges to a Cantor set, whose measure is zero. Consequently, it is nearly impossible to observe non-periodic behaviors if there is no uncertainty.

4 Chaotic motions under imperfect observation

In this section, we investigate the dynamic behaviors of the model that incorporates uncertainty, which is represented by equation (10). We first show that this model has the Markov property under some parameter values, which allows the observation of chaotic dynamics in the long run. Furthermore, the chaotic trajectories can be characterized by invariant densities.

4.1 Markov property

First of all, the notion of a Markov partition should be discussed. Let $I = [0,1]$ and $f : I \to I$ be a mapping of I onto itself. Divide the unit interval into subintervals I_i by a finite partition $\mathcal{P}$. If f_i is a homeomorphism from I_i onto some connected union of intervals of $\mathcal{P}$, then f is said to be Markov. The partition is said to be a Markov partition with respect to f. See, for example, Boyarsky and Gora (1997) for more details.

Proposition 1. *(Observable chaos on a period-5 Markov partition) If $\theta_L = \theta_{5,L}$, $\theta_R = \theta_{5,R}$, $a = \hat{a} = a(\theta_{5,L}, \theta_{5,R})$ and $\sigma = \hat{\sigma} = \sigma(\hat{a})$, then φ defined by (10) has a period-5 Markov partition of the unit interval and exhibits observable chaos.*

Proof. First, we show that the model (10) can exhibit the following period-5 cycle:

$$0 = \varphi^5(0) < \theta_{5,L} = \varphi^2(0) < \theta_{5,R} = \varphi^4(0) < \gamma = \varphi(0) < \varphi^3(0) = 1, \tag{11}$$

which is illustrated in Fig. 6. To calculate this period-5 cycle, we need that $\theta_{5,L}$ and $\theta_{5,R}$ satisfy

$$\varphi_R(\varphi_L(0)) = \theta_{5,L}, \qquad \varphi_R(1) = \theta_{5,R}.$$

By solving the above two equations for $\theta_{5,L}$ and $\theta_{5,R}$, we can obtain

$$\theta_{5,L} = \frac{b}{(1+b)(1+ab)}, \qquad \theta_{5,R} = \frac{b}{1+b}. \tag{12}$$

Further calculation shows that $\theta_{5,R} - \theta_{5,L} = ab^2/(1+b+ab+ab^2)$.

Specially, using equations (6), (8), and (12) to solve $\theta_L(\sigma, a) = \theta_{5,L}$ and $\theta_R(\sigma, a) = \theta_{5,R}$ for a and σ, we derive particular $\hat{a}$ and $\hat{\sigma}$. Note that the specific expression for $\hat{a}$ is omitted here for brevity, but $\hat{\sigma}$ can be expressed as follows:

$$\hat{\sigma} = \sigma(\hat{a}) = \frac{\hat{a}b(1-b-c)}{(2+\hat{a}b+\hat{a}b^2)(\hat{a}-b-c)}.$$

See the appendix for detailed computation of $\hat{a}$ and $\hat{\sigma}$. Moreover, it can be verified that $\hat{\sigma}$ satisfies the constraint (7) as the following inequality always holds:

$$\frac{\hat{a}b(1-b-c)}{2+\hat{a}b+\hat{a}b^2} < 1.$$

Next, we show that φ is eventually expanding. Let $I_1 = (0, \theta_{5,L})$, $I_2 = (\theta_{5,L}, \theta_{5,R})$, $I_3 = (\theta_{5,R}, \gamma)$, and $I_4 = (\gamma, 1)$. Then one can easily confirm that

$$\varphi^3(I_1) = \varphi(I_2) = \varphi^4(I_3) = \varphi^2(I_4) = I.$$

Since every point $x \in \cup_{i=1}^4 I_i$ will visit I_1 at least once every fourth iteration, it will also visit I_2 at least once every fourth iteration. Therefore,

$$|(\varphi^4)'(x)| \geq |\varphi'_L| \cdot |\varphi'_M| \cdot |\varphi'_R|^2 = \frac{\hat{a}b^2}{|\theta_{5,R} - \theta_{5,L}|} = 1 + b + \hat{a}b + \hat{a}b^2 > 1.$$

Note that $|\varphi'_L||\varphi'_M||\varphi'_R|^2$ is the smallest possible case. Although $|\varphi'_R|^3|\varphi'_M|$ yields a smaller numerical value, it is logically impossible for such a case to occur.

Since $|(\varphi^4)'(x)| > 1$, the map φ given by (10) is eventually expanding, which implies that the map exhibits observable chaos. □

Proposition 2. *(Observable chaos on a period-7 Markov partition) If $\theta_L = \theta_{7,L}$, $\theta_R = \theta_{7,R}$, $a = \hat{a} = a(\theta_{7,L}, \theta_{7,R})$ and $\sigma = \hat{\sigma} = \sigma(\hat{a})$, then φ defined by* (10) *has a period-7 Markov partition of the unit interval and exhibits observable chaos.*

Proof. There is a period-7 cycle as follows:

$$\begin{aligned} 0 = \varphi^7(0) < \theta_{7,L} = \varphi^3(0) < \theta_{7,R} = \varphi^6(0) \\ < \varphi^2(0) < \varphi^5(0) < \varphi(0) < \varphi^4(0) = 1. \end{aligned}$$

Fig. 7 illustrates this period-7 Markov partition. By solving $\varphi_R^2(\varphi_L(0)) = \theta_{7,L}$ and $\varphi_R^2(1) = \theta_{7,R}$, we can obtain

$$\theta_{7,L} = \frac{b^2}{(1+b+b^2)(1+ab^2)}, \qquad \theta_{7,R} = \frac{b^2}{1+b+b^2}. \tag{13}$$

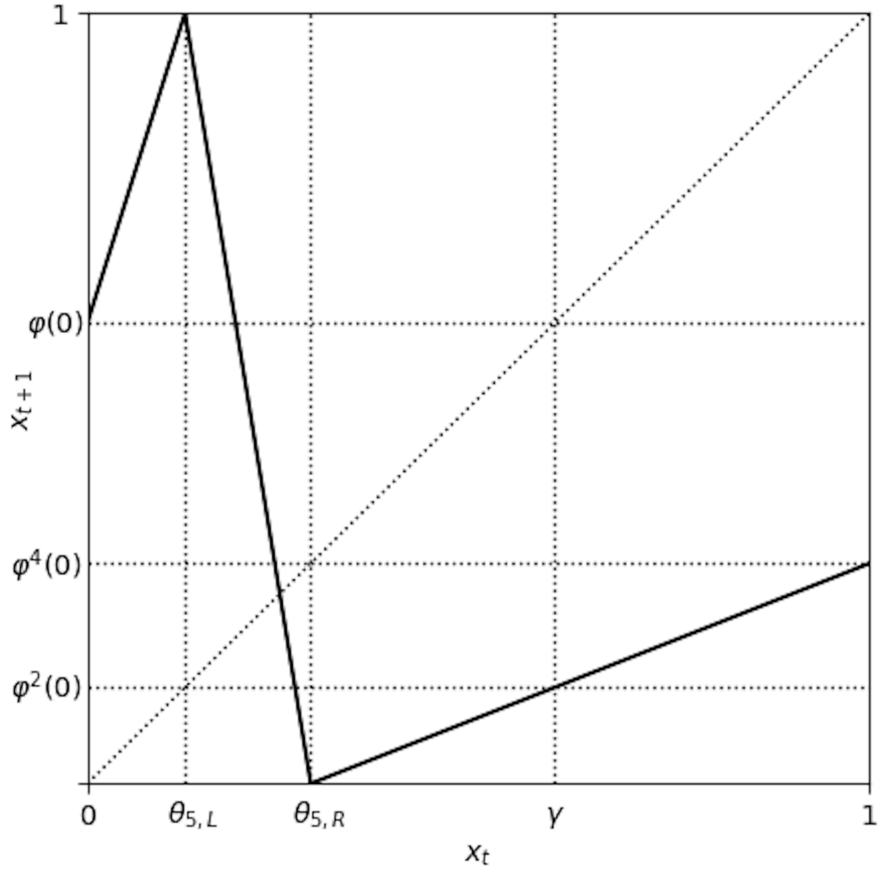

Figure 6: Period-5 Markov property. $n = 0, \delta = 1, s = 0.2, A_2 = 2.5, \alpha = 0.8, \hat{A}_1 \approx 16.09, \hat{\sigma} \approx 0.06$.

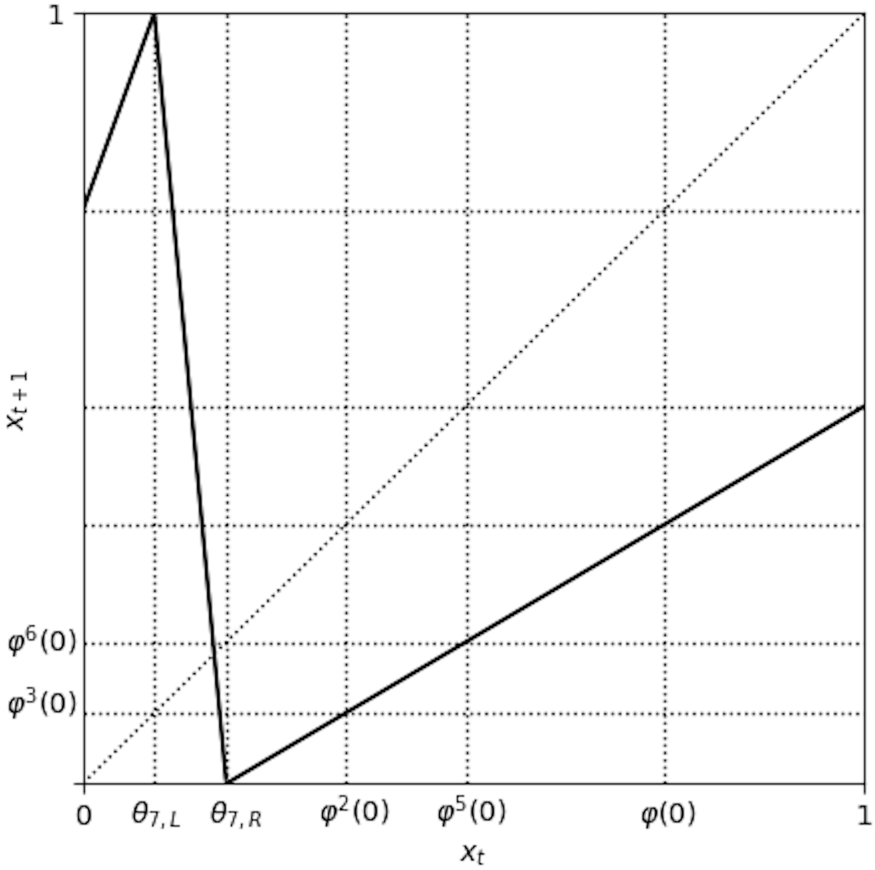

Figure 7: Period-7 Markov property. $n = 0, \delta = 1, s = 0.2, A_2 = 3.5, \alpha = 6/7, \hat{A}_1 \approx 14, \hat{\sigma} \approx 0.04$.

Note that $\theta_{7,R} - \theta_{7,L} = ab^4/[(1+b+b^2)(1+ab^2)]$. Furthermore, by solving $\theta_L(\sigma, a) = \theta_{7,L}$ and $\theta_R(\sigma, a) = \theta_{7,R}$ for a and σ, we obtain specific $\hat{a}$ and $\hat{\sigma}$. It can also be verified that $\hat{\sigma}$ satisfies the constraint (7).

Let $I_1 = (0, \theta_{7,L})$, $I_2 = (\theta_{7,L}, \theta_{7,R})$, $I_3 = (\theta_{7,R}, \varphi^2(0))$, $I_4 = (\varphi^2(0), \varphi^5(0))$, $I_5 = (\varphi^5(0), \varphi(0))$, and $I_6 = (\varphi(0), 1)$. Then it is easy to confirm that

$$\varphi^4(I_1) = \varphi(I_2) = \varphi^5(I_3) = \varphi^2(I_4) = \varphi^6(I_5) = \varphi^3(I_6) = I.$$

Since every point $x \in \cup_{i=1}^{6} I_i$ will visit I_1 at least once every sixth iteration, it will also visit I_2 at least once every sixth iteration. Therefore,

$$|(\varphi^6)'(x)| \geq |\varphi_L'| \cdot |\varphi_R'|^4 \cdot |\varphi_M'| = \frac{\hat{a}b^4}{|\theta_{7,R} - \theta_{7,L}|} = (1+b+b^2)(1+\hat{a}b^2) > 1.$$

□

From Proposition 1 and Proposition 2, the more general case summarized in Proposition 3 can be obtained.

Proposition 3. *(Observable chaos on a period-(2n+3) Markov partition) If* $\theta_L = \theta_{2n+3,L}$*,* $\theta_R = \theta_{2n+3,R}$*,* $a = \hat{a} = a(\theta_{2n+3,L}, \theta_{2n+3,R})$ *and* $\sigma = \hat{\sigma} = \sigma(\hat{a})$*, then* φ *defined by* (10) *has a period-(2n+3) Markov partition of the unit interval and exhibits observable chaos.*

Proof. Solve

$$\varphi_R^n(\varphi_L(0)) = \theta_{2n+3,L}, \qquad \varphi_R^n(1) = \theta_{2n+3,R}$$

to have a period $2n+3$. This yields

$$\theta_{2n+3,L} = \frac{b^n(1-b)}{(1-b^{n+1})(1+ab^n)}, \qquad \theta_{2n+3,R} = \frac{b^n(1-b)}{1-b^{n+1}}. \tag{14}$$

Further calculation shows that $\theta_{2n+3,R} - \theta_{2n+3,L} = [ab^{2n}(1-b)]/[(1-b^{n+1})(1+ab^n)]$. By an analogous method, we obtain $\hat{a}$ and $\hat{\sigma}$ by solving $\theta_L(\sigma, a) = \theta_{2n+3,L}$ and $\theta_R(\sigma, a) = \theta_{2n+3,R}$. See the appendix for computation of $\hat{a}$ and $\hat{\sigma}$.

We show that φ is eventually expanding as follows. Since every point $x \in \cup_{i=1}^{2n+2} I_i$ will visit I_1 at least once every $(2n+2)$th iteration, it will also visit I_2 at least once every $(2n+2)$th iteration. Therefore,

$$|(\varphi^{2n+2})'(x)| \geq |\varphi_L'| \cdot |\varphi_R'|^{2n} \cdot |\varphi_M'| = (1+\hat{a}b^n)(1+b+\cdots+b^n) > 1.$$

□

4.2 Predictable chaos on a Markov partition

We know that φ defined by (10) is a piecewise linear Markov transformation. This allows us to calculate the long-run distribution of chaotic trajectories, making erratic business cycles predictable. See, for example, Matsumoto (2005) for the construction of invariant density functions.

Before proceeding with the analysis, we first introduce a matrix version of the Frobenius–Perron operator, $M_\varphi = (m_{ij})_{1 \leq i,j \leq n}$, the entries of which are given by

$$m_{ij} = \frac{q_{ij}}{|\varphi_i'|}, \qquad 1 \leq i, j \leq n,$$

where $Q_\varphi = (q_{ij})_{1\le i,j\le n}$ is the incidence matrix induced by piecewise monotonic transformation φ and partition $\mathcal{P}$ of I. More specifically,

$$q_{ij} = \begin{cases} 1, & \text{if} \quad I_j \subset \varphi(I_i), \\ 0, & \text{otherwise.} \end{cases}$$

For more details, see Boyarsky and Gora (1997) or Boyarsky and Scarowsky (1979).

Proposition 4. *(Invariant density on a period-5 Markov partition) If φ is Markov on $\{I_i\}_{i=1}^4$, inf $|(\varphi^4)'| > 1$, and matrix $M_\varphi = M_{\varphi_5}$, then φ admits an invariant density function $\pi = \pi_5^*(x)$, and the corresponding probability density is $p(x) = \pi_5^*(x)/\sum_{i=1}^4 \pi_i|I_i|$.*

Proof. From the previous subsection, for a period-5 Markov partition, the following relationship holds:

$$I_4 \subset \varphi(I_1), \quad \cup_{i=1}^4 I_i \subset \varphi(I_2), \quad I_1 \subset \varphi(I_3), \quad I_2 \subset \varphi(I_4).$$

Then, the 4×4 matrix induced by φ is

$$M_{\varphi_5} = \begin{bmatrix} 0 & 0 & 0 & \frac{1}{a} \\ \triangle & \triangle & \triangle & \triangle \\ \frac{1}{b} & 0 & 0 & 0 \\ 0 & \frac{1}{b} & 0 & 0 \end{bmatrix}.$$

where $\triangle = ab^2/[(1+b)(1+ab)]$ and $a = \hat{a} = a(\theta_{5,L}, \theta_{5,R})$.

Since we know that φ is Markov on $\{I_i\}_{i=1}^4$ and that inf $|(\varphi^4)'| > 1$ from the previous subsection, by Theorem 9.4.2 of Boyarsky and Gora (1997), φ admits an invariant density which is the nontrivial solution of $\pi M_{\varphi_5} = \pi$, that is, the left eigenvector for eigenvalue 1. Therefore, the following defines the invariant density function $\pi_5^*(x)$:

$$\pi_5^*(x) = \begin{cases} \hat{a}b + \hat{a}b^2 \equiv \pi_1, & x \in I_1 \\ \hat{a}b^2 + \hat{a}b + 1 + b \equiv \pi_2, & x \in I_2 \\ \hat{a}b^2 \equiv \pi_3, & x \in I_3 \\ \hat{a}b^2 + b + b^2 \equiv \pi_4, & x \in I_4 \end{cases}.$$

□

The corresponding probability density, the normalized invariant density, is illustrated in Fig. 8. The area for interval I_i represents the frequency that a typical chaotic trajectory visits I_i.

It is also worth noting that the mean $\mu = \mu(\hat{a}, b)$ and standard deviation $\omega = \omega(\hat{a}, b)$ of chaotic trajectories can be obtained by straightforward computations (see the appendix). For instance, when $b = 0.4$, $c = 0.1$, we find $\hat{a} \approx 3.22$, $\hat{\sigma} = 0.06$, and subsequently calculate $\mu \approx 0.4022$ and $\omega \approx 0.3035$. In particular, theoretical values and estimated values converge asymptotically.

Proposition 5. *(Invariant density on a period-7 Markov partition) If φ is Markov on $\{I_i\}_{i=1}^6$, inf $|(\varphi^6)'| > 1$, and matrix $M_\varphi = M_{\varphi_7}$, then φ admits an invariant density function $\pi = \pi_7^*(x)$ and the corresponding probability density is $p(x) = \pi_7^*(x)/\sum_{i=1}^6 \pi_i|I_i|$.*

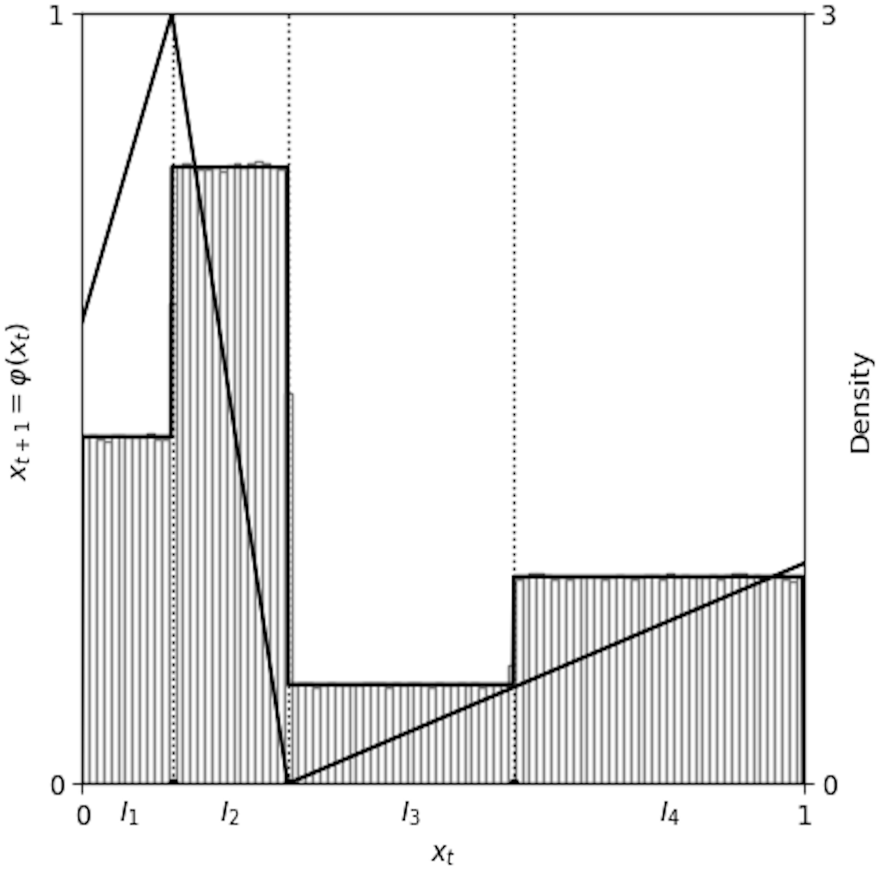

Figure 8: Invariant density for the period-5 Markov map. $n = 0, \delta = 1, s = 0.2, A_2 = 2.5, \alpha = 0.8, \hat{A}_1 \approx 16.09, \hat{\sigma} \approx 0.06$. Density $p(x) = \pi_5^*(x)/\sum_{i=1}^4 \pi_i |I_i|$. Simulated histogram of 10^6 iterations.

Proof. Using an analogous method to that for the invariant density on a period-5 Markov partition case, we first obtain the following relationships:

$$I_6 \subset \varphi(I_1),\ \cup_{i=1}^{6} I_i \subset \varphi(I_2),\ I_1 \subset \varphi(I_3),\ I_2 \subset \varphi(I_4),\ I_3 \subset \varphi(I_5),\ I_4 \subset \varphi(I_6).$$

Then, a 6×6 matrix is obtained as follows:

$$M_{\varphi_7} = \begin{bmatrix} 0 & 0 & 0 & 0 & 0 & \frac{1}{a} \\ \triangle & \triangle & \triangle & \triangle & \triangle & \triangle \\ \frac{1}{b} & 0 & 0 & 0 & 0 & 0 \\ 0 & \frac{1}{b} & 0 & 0 & 0 & 0 \\ 0 & 0 & \frac{1}{b} & 0 & 0 & 0 \\ 0 & 0 & 0 & \frac{1}{b} & 0 & 0 \end{bmatrix},$$

where $\triangle = \theta_{7,R} - \theta_{7,L} = ab^4/[(1+b+b^2)(1+ab^2)]$ and $a = \hat{a} = a(\theta_{7,L}, \theta_{7,R})$.

The corresponding invariant density $\pi_7^*(x)$ can be calculated as

$$\pi_7^*(x) = \begin{cases} \hat{a}b^4 + \hat{a}b^3 + \hat{a}b^2, & x \in I_1 \\ \hat{a}b^4 + \hat{a}b^3 + \hat{a}b^2 + b^2 + b + 1, & x \in I_2 \\ \hat{a}b^4 + \hat{a}b^3, & x \in I_3 \\ \hat{a}b^4 + \hat{a}b^3 + b^3 + b^2 + b, & x \in I_4 \\ \hat{a}b^4, & x \in I_5 \\ \hat{a}b^4 + b^4 + b^3 + b^2, & x \in I_6 \end{cases}.$$

□

The corresponding probability density is depicted in Fig. 9.

To find the general form of invariant density, we also calculate $\pi_9^*(x)$ for $n = 3$. See the appendix for the computation of $\pi_9^*(x)$, where the corresponding probability density is $p(x) = \pi_9^*(x)/\sum_{i=1}^{8} \pi_i |I_i|$.

Proposition 6. *(Invariant density on a period-(2n+3) Markov partition) If φ is Markov on $\{I_i\}_{i=1}^{2n+2}$, $inf|(\varphi^{2n+2})'| > 1$, and matrix $M_\varphi = M_{\varphi_{2n+2}}$, then φ admits an invariant density function $\pi = \pi_{2n+3}^*(x)$ and its corresponding probability density is $p(x) = \pi_{2n+3}^*(x)/\sum_{i=1}^{2n+2} \pi_i |I_i|$.*

Proof. By the same argument, we can obtain the following $(2n+2) \times (2n+2)$ matrix:

$$M_{\varphi_{2n+3}} = \begin{bmatrix} 0 & 0 & \cdots & 0 & 0 & \frac{1}{a} \\ \triangle & \triangle & \cdots & \triangle & \triangle & \triangle \\ \frac{1}{b} & 0 & \cdots & 0 & 0 & 0 \\ 0 & \frac{1}{b} & \cdots & 0 & 0 & 0 \\ \vdots & \vdots & \ddots & \vdots & \vdots & \vdots \\ 0 & 0 & \cdots & \frac{1}{b} & 0 & 0 \end{bmatrix}.$$

Here, $\triangle = \theta_{2n+3,R} - \theta_{2n+3,L} = [ab^{2n}(1-b)]/[(1-b^{n+1})(1+ab^n)]$ and $a = \hat{a} = a(\theta_{2n+3,L}, \theta_{2n+3,R})$.

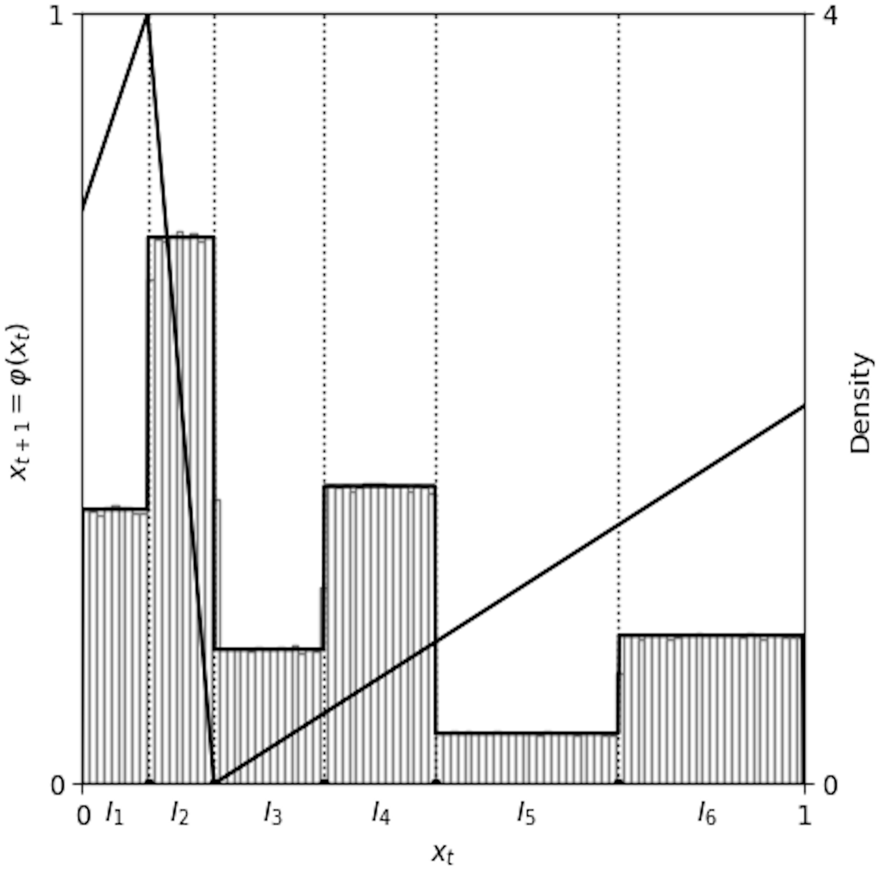

Figure 9: Invariant density for the period-7 Markov map. $n = 0, \delta = 1, s = 0.2, A_2 = 3.5, \alpha = 6/7, \hat{A}_1 \approx 14, \hat{\sigma} \approx 0.04$. Density $p(x) = \pi_7^*(x)/\sum_{i=1}^{6} \pi_i |I_i|$. Simulated histogram of 10^6 iterations.

Then, solving $\pi M_{\varphi_{2n+2}} = \pi$, we obtain

$$\pi^*_{2n+3}(x) = \begin{bmatrix} \pi_1 \\ \pi_2 \\ \vdots \\ \pi_{2n+1} \\ \pi_{2n+2} \end{bmatrix}.$$

Here, $\pi_2 = (1 + \hat{a}b^n)(1 + b + \cdots + b^n)$, which is the maximum, and $\pi_{2n+1} = \hat{a}b^{2n}$, which is the minimum. If the Markov partition can be split into odd and even terms, it is possible to derive the remaining items from π_2 and π_{2n+1}. □

5 Conclusion

We have developed a regime-switching model that can exhibit periodic fluctuations and chaotic dynamics. The two distinct regimes and endogenous cycles are from the binary choice of production technology. In addition, chaotic motions are induced by observation errors. More importantly, the chaos was characterized by the Markov property, which allows the calculation of invariant densities. It is, thus, possible to predict the highly erratic trajectories in the long run.

We give here a few notes on technology choice and observation errors. Technology choice here can be interpreted more broadly. For example, if the output is taken abstractly, then technology choice may be described as the choice of industry in which investors (shareholders) invest. Or, to take a slight leap forward, it may be regarded as the choice of the political party supported by investors (such as between the two major parties, the Republican and Democratic parties, in the United States of America). This is because one can imagine that the party in power will have an impact on the macro structure of production.

As for the observation errors introduced here, there may be other interpretations. For instance, we could assume that there is some heterogeneity among firms so that their optimal thresholds vary even if no observation errors are present.

Finally, the piecewise linear model presented here is based on very specific parameters and a very specific distribution of observation errors. In this very special situation, the chaotic dynamics of the model, usually considered unpredictable, become predictable because they are fully described in some probabilistic sense. Therefore, it remains to be seen whether the model with the Markov property has some robustness. If so, the Solow model with the Markov property could be regarded as a good benchmark. This topic is, however, left for future research.

Appendix A. Proof of $0 < \theta < 1$

From the right-hand inequality of $A_1 > (n + \delta)/s > A_2$, we have

$$\frac{n+\delta}{sA_1} > \frac{A_2}{A_1}.$$

This implies

$$\frac{n+\delta-sA_2}{sA_1} > 0.$$

Since

$$\theta = \frac{n+\delta - sA_2}{s(A_1 - A_2)} > \frac{n+\delta - sA_2}{sA_1},$$

it is clear that $\theta > 0$.

On the other hand, since $sA_1 > n + \delta$, the operation of finding a common denominator yields

$$\frac{n+\delta - sA_2}{s(A_1 - A_2)} < \frac{n+\delta}{sA_1}.$$

From the left-hand inequality of $A_1 > (n+\delta)/s > A_2$, we have

$$\frac{n+\delta}{sA_1} < 1.$$

Hence, we can verify that $\theta < 1$.

Appendix B. Computation of G_M

The explicit forms of $h(k_t)$ and $\varphi_M(x_t)$ give us

$$x_{t+1} = \varphi_M(h(k_t)) = \frac{k_R - k_t}{k_R - k_L}.$$

Consequently,

$$k_{t+1} = h^{-1}(x_{t+1}) = h^{-1}(\varphi_M(h(k_t))) = [ak_L - (bk_R + c)] \cdot \frac{k_R - k_t}{k_R - k_L} + (bk_R + c).$$

On the other hand, using equation (4), G_M can be obtained as follows:

$$G(\rho(k_t)) = \frac{k_L(a-b) - c}{k_t(a-b) - c} \cdot \frac{k_R - k_t}{k_R - k_L}.$$

Since $k_t = \rho^{-1}(y_t)$, equation (9) can be obtained by substitution.

Appendix C. Computation of $(\hat{\sigma},\ \hat{a})$

From equations (6) and (8), we can obtain

$$\theta_L(\sigma, a) = \frac{1 - b - c - \sigma(a-b-c)(1+b)}{a - b - c - \sigma(a-b-c)(a+b)} \quad \text{and}$$
$$\theta_R(\sigma, a) = \frac{1 - b - c + \sigma(a-b-c)(1-b)}{a - b - c - \sigma(a-b-c)(a+b)}.$$

To derive $\hat{\sigma}$ and $\hat{a}$, we solve $\theta_L(\sigma, a) = \theta_{5,L}$ and $\theta_R(\sigma, a) = \theta_{5,R}$ using equation (12). Given b and c, $\hat{a}$ can be attained by solving

$$\frac{(1-b-c)(1+ab) - (ab-1+c)(1+b)}{(a-b-c)(1+ab) - (ab-1+c)(a+b)} = \frac{b}{(1+b)(1+ab)}.$$

for a. For brevity, the explicit expression of $\hat{a}$ is not presented here, but it can be solved since this is a quadratic equation in terms of a. Based on this $\hat{a}$, we solve

$$\frac{1-b-c-\sigma(\hat{a}-b-c)(1+b)}{\theta_{5,L}} = \frac{1-b-c+\sigma(\hat{a}-b-c)(1-b)}{\theta_{5,R}}.$$

for $\hat{\sigma}$, from the equation (12), $\hat{\sigma} = \sigma(\hat{a})$ can be obtained, as indicated in the main text.

For the general case, we solve $\theta_L(\sigma, a) = \theta_{2n+3,L}$ and $\theta_R(\sigma, a) = \theta_{2n+3,R}$ for $\hat{a}$ and $\hat{\sigma}$ to find that $\hat{a}$ can be obtained from

$$\frac{(1-b-c)D_1 - (1+b)D_2}{(a-b-c)D_1 - (a+b)D_2} = \frac{b^n(1-b)}{(1-b^{b+1})(1+ab^n)},$$

where $D_1 = (1-b)(1+ab^n)$ and $D_2 = b^n(1-b)(a-b-c) - (1-b^{n+1})(1-b-c)$.

Given this $\hat{a}$, a particular $\hat{\sigma}$ can be obtained as follows:

$$\hat{\sigma} = \sigma(\hat{a}) = \frac{\hat{a}b^n(1-b-c)}{(\hat{a}-b-c)(2+\hat{a}b^n+\hat{a}b^{n+1})}.$$

Appendix D. Computation of μ and ω

From the probability density, the mean μ is calculated as

$$\begin{aligned}
\mu &= \int_I x \cdot p(x)\, dx \\
&= \int_I x \cdot \frac{\pi_5^*(x)}{\sum_{i=1}^4 \pi_i |I_i|}\, dx \\
&= \frac{\pi_1 \cdot \theta_{5,L}^2 + \pi_2 \cdot (\theta_{5,R}^2 - \theta_{5,L}^2) + \pi_3 \cdot (\gamma^2 - \theta_{5,R}^2) + \pi_4 \cdot (1-\gamma^2)}{2\sum_{i=1}^4 \pi_i |I_i|} \\
&= \frac{3 + 9b + 5b^2 + 3\hat{a}b + 10\hat{a}b^2 + 5\hat{a}b^3 + \hat{a}^2b^2 + 3\hat{a}^2b^3 + \hat{a}^2b^4}{2(4+3b+2\hat{a}b+\hat{a}b^2)(1+b)(1+\hat{a}b)} \\
&= \mu(\hat{a}, b),
\end{aligned}$$

where $\hat{a} = a(\theta_{5,L}, \theta_{5,R})$. To obtain the standard derivation ω, it is necessary to calculate the variance ω^2.

$$\begin{aligned}
\omega^2 &= \int_I (x-\mu)^2 \cdot p(x)\, dx \\
&= \int_I x^2 \cdot p(x)\, dx - \mu^2 \\
&= \frac{\pi_1 \cdot \theta_{5,L}^3 + \pi_2 \cdot (\theta_{5,R}^3 - \theta_{5,L}^3) + \pi_3 \cdot (\gamma^3 - \theta_{5,R}^3) + \pi_4 \cdot (1-\gamma^3)}{3\sum_{i=1}^4 \pi_i |I_i|} - \mu^2.
\end{aligned}$$

Therefore, the standard derivation $\omega = \omega(\hat{a}, b)$ is the square root of the above.

Appendix E. Computation of $\pi_9^*(x)$

From M_{φ_5} and M_{φ_7}, we can obtain M_{φ_9}, which is an 8×8 matrix.

$$M_{\varphi_9} = \begin{bmatrix} 0 & 0 & 0 & 0 & 0 & 0 & 0 & \frac{1}{a} \\ \triangle & \triangle & \triangle & \triangle & \triangle & \triangle & \triangle & \triangle \\ \frac{1}{b} & 0 & 0 & 0 & 0 & 0 & 0 & 0 \\ 0 & \frac{1}{b} & 0 & 0 & 0 & 0 & 0 & 0 \\ 0 & 0 & \frac{1}{b} & 0 & 0 & 0 & 0 & 0 \\ 0 & 0 & 0 & \frac{1}{b} & 0 & 0 & 0 & 0 \\ 0 & 0 & 0 & 0 & \frac{1}{b} & 0 & 0 & 0 \\ 0 & 0 & 0 & 0 & 0 & \frac{1}{b} & 0 & 0 \end{bmatrix},$$

where $\triangle = \theta_{9,R} - \theta_{9,L} = ab^6/[(1+b)(1+b^2)(1+ab^3)]$. Using M_{φ_9}, we can calculate

$$\pi_9^*(x) = \begin{bmatrix} ab^6 + ab^5 + ab^4 + ab^3 \\ ab^6 + ab^5 + ab^4 + ab^3 + b^3 + b^2 + b + 1 \\ ab^6 + ab^5 + ab^4 \\ ab^6 + ab^5 + ab^4 + b^4 + b^3 + b^2 + b \\ ab^6 + ab^5 \\ ab^6 + ab^5 + b^5 + b^4 + b^3 + b^2 \\ ab^6 \\ ab^6 + b^6 + b^5 + b^4 + b^3 \end{bmatrix}.$$

Here we note that $a = \hat{a} = a(\theta_{9,L}, \theta_{9,R})$, which is the solution to $\theta_L(\sigma, a) = \theta_{9,L}$ and $\theta_R(\sigma, a) = \theta_{9,R}$.

References

Agliari, A., Böhm, V., Pecora, N. (2020). Endogenous cycles from income diversity, capital ownership, and differential savings. *Chaos, Solitons and Fractals*, 130: 109435.

Asano, T., Shibata, A., Yokoo, M. (2022). Quasi-periodic motions in a two-class economy with technology choice: an extreme case. *Nonlinear Dynamics*, 110: 945–961.

Asano, T., Yokoo, M. (2019). Chaotic dynamics of a piecewise linear model of credit cycles. *Journal of Mathematical Economics*, 80: 9–21.

Beaudry, P., Galizia, D., Portier, F. (2020). Putting the cycle back into business cycle analysis. *American Economic Review*, 110: 1–47.

Böhm, V., Kaas, L. (2000). Differential savings, factor shares, and endogenous growth cycles. *Journal of Economic Dynamics & Control*, 24: 965–980.

Boyarsky, A., Gora, P. (1997). *Laws of Chaos: Invariant Measures and Dynamical Systems in One Dimension*. Springer.

Boyarsky, A., Scarowsky, M. (1979). On a class of transformations which have unique absolutely continuous invariant measures. *Transactions of the American Mathematical Society*, 255: 243-262.

Chen, K., Gong, X., Marcus, R.D. (2014). The new evidence to tendency of convergence in Solow model. *Economic Modelling*, 41: 263–266.

Keener, J.P. (1980). Chaotic behavior in piecewise continuous difference equations. *Transactions of the American Mathematical Society*, 261: 589-604.

Kufenko, V., Prettner, K., Geloso, V. (2020). Divergence, convergence, and the history-augmented Solow model. *Structural Change and Economic Dynamics*, 53: 62-76.

Matsumoto, A. (2005). Density function of piecewise linear transformation. *Journal of Economic Behavior & Organization*, 56: 631-653.

Solow, R.M. (1956). A contribution to the theory of economic growth. *The Quarterly Journal of Economics*, 70: 65-94.

Sushko, I., Commendatore, P., Kubin, I. (2020). Codimension-two border collision bifurcation in a two-class growth model with optimal saving and switch in behavior. *Nonlinear Dynamics*, 102: 1071-1095.

Umezuki, Y., Yokoo, M. (2019). A simple model of growth cycles with technology choice. *Journal of Economic Dynamics & Control* , 100: 164–175.

Yokoo, M., Ishida, J. (2008). Misperception-driven chaos: Theory and policy implications. *Journal of Economic Dynamics & Control* , 32: 1732–1753.